NUCLEAR INSTRUMENTS AND METHODS 51 (1967) 325–338; © NORTH-HOLLAND PUBLISHING CO.

STATISTICAL BEHAVIOUR OF THE SCINTILLATION COUNTER: EXPERIMENTAL RESULTS

M. BERTOLACCINI†, C. BUSSOLATI and S. COVA†

Istituto di Fisica Sperimentale, Politecnico di Milano, Italy

and

S. DONATI* and V. SVELTO+

Laboratori CISE, Segrate, Milano, Italy

Received 7 December 1966

We have done an experimental test of a theory of the scintillation detector's statistical properties. Mean and amplitude variance of the output current pulse following γ-rays excitation, have been calculated and measured. We have taken into account the case of non-Poissonian photoelectron distribution and considered the effect on the mean and variance of the output current pulse of amplitude selection of the charge pulses from the scintillation detector. To test the theory, we have measured: the equivalent illumination, the single electron response, the gain of the electronmultiplier and its variance, the mean and variance of the selected output charge distribution.

From these measurements, mean and variance of the output current pulse as a function of time have been calculated and compared with the same quantities measured directly.

The good agreement between theoretical and experimental results support our theoretical model for the behaviour of the scintillation counter. We can conclude that to describe the statistical behaviour of the scintillation counter it is sufficient to know the following parameters: equivalent illumination, single electron response, gain of the electronmultiplier and its variance, mean and variance of the selected output spectrum.

1. Introduction

The statistical properties of a scintillation detector set a limit to the accuracy achievable both in energy and in time measurements in nuclear physics.

Theoretical investigations of the problem are available, with different approximations, from several works[1,2,7]). Recently, it has been shown that a solution can be obtained by a rigorous statistical method[3]) applied to a fairly general model of the scintillation detector. The exact solution obtained in this way has been also useful in evaluating the degree of approximation of a preceding theory[1,2]), proving its adequacy for describing the statistical behaviour of the scintillation detector.

Our aim has been a direct experimental check of the theory; in fact, experimental results obtained until now, though not in complete disagreement with theoretical data, do not give a satisfactory proof of the validity of the used statistical model; this may depend on their being a by-product of amplitude and time measurements.

Let us briefly recall the main results of the theory we intend to verify; for a detailed treatment of the subject we refer to a preceding paper[2]).

The statistical properties of the signals from the scintillation detector can be described by the equivalent illumination $I(t)$ and by the single electron response (SER), $f(t)$. $I(t)$ is defined as the probability density function (pdf) of the arrival of an electron at the first dynode of the electronmultiplier, following an event detected, at time $t=0$, by the scintillator; $f(t)$ is the average response at the output of the photomultiplier due to an electron impinging at time $t=0$ on the first dynode.

With this model, the output current pulse $S(t)$, considered as a random function, is characterized by a mean shape $\bar{S}(t)$ and a variance $\varepsilon_S^2(t)$ given by:

$$\bar{S}(t) = R\int_0^t I(\tau)f(t-\tau)\,\mathrm{d}\tau, \qquad (1)$$

$$\varepsilon_S^2(t) = (1+\varepsilon_A^2)R\int_0^t I(\tau)f^2(t-\tau)\,\mathrm{d}\tau. \qquad (2)$$

The expressions (1) and (2) are valid under the assumption that an event releases an average of N Poisson distributed photons, the photoelectric conversion being described by a Bernouilli distribution with success probability p, so that the resulting photoelectron distribution is Poissonian with mean value $R = Np$. ε_A^2 in expression (2) is the relative variance of the total gain of the electronmultiplier. For what follows, we will refer to this case as the Poissonian one. It is well known that the energy released within a scintillator by a nuclear event has a continuous distribution even in the case of monoenergetic radiation (Compton effect, particularly important in organic scintillators). As a consequence, in such cases, the distribution of the number of photoelectrons is not Poissonian; it can be

* Consiglio Nazionale delle Ricerche (CNR).
+ Laboratori CISE and Università di Milano.
† I.N.F.N. (Gruppo Politecnico, Milano).

described as the sum of Poisson distributions with different average values. Moreover an amplitude selection performed at the output of the detector, e.g. by mean of a SCA, is generally not equivalent to selecting a given value of R with its Poisson distribution.

In the appendix we give the theory relative to the most general case of amplitude selection at the output; we find that formula (1) is still formally valid:

$$\bar{S}(t) = R_f \int_0^t I(\tau) f(t-\tau)\,\mathrm{d}\tau, \qquad (1a)$$

provided one takes for R_f the number of photoelectrons corresponding to the mean of the distribution selected by the SCA; the formula corresponding to eq. (2), is:

$$\varepsilon_S^2(t) = (1+\varepsilon_A^2) R_f \int_0^t I(\tau) f^2(t-\tau)\,\mathrm{d}\tau + \{\varepsilon_f^2 - (1+\varepsilon_A^2)/R_f\}\bar{S}^2(t), \qquad (2a)$$

where ε_f^2 is the relative variance of the distribution selected by the SCA.

With the normally employed values of R_f and ε_f^2, defined by the SCA, the second term of eq. (2a) gives a negative contribution. As a consequence the amplitude variance observed when selecting by means of a SCA, is less than the one observed in the case we called Poissonian, for which formulas (1) and (2) are valid.

As pointed out in a preceding paper[2]) the variance $\varepsilon_t^2(t)$ of the crossing time of an ideal threshold is given by the ratio of the amplitude variance to the square of the slope of the mean pulse:

$$\varepsilon_t^2(t) = \varepsilon_S^2(t)/[\mathrm{d}\bar{S}(t)/\mathrm{d}t]^2. \qquad (3)$$

2. Experimental measurements

We experimentally tested the validity of formulas (1a) and (2a). This was done by measuring directly the equivalent illumination $I(t)$, the SER $f(t)$, the selected distribution and its parameters R_f and ε_f^2.

For the sake of simplicity ε_A^2 has been derived from a measurement of the gain of the electronmultiplier. In the case of secondary multiplication factor g equal for all dynodes, we have $\varepsilon_A^2 = 1/(g-1)$.

This parameter could be directly measured from a determination of the amplitude distribution[4]) of the area of the SER.

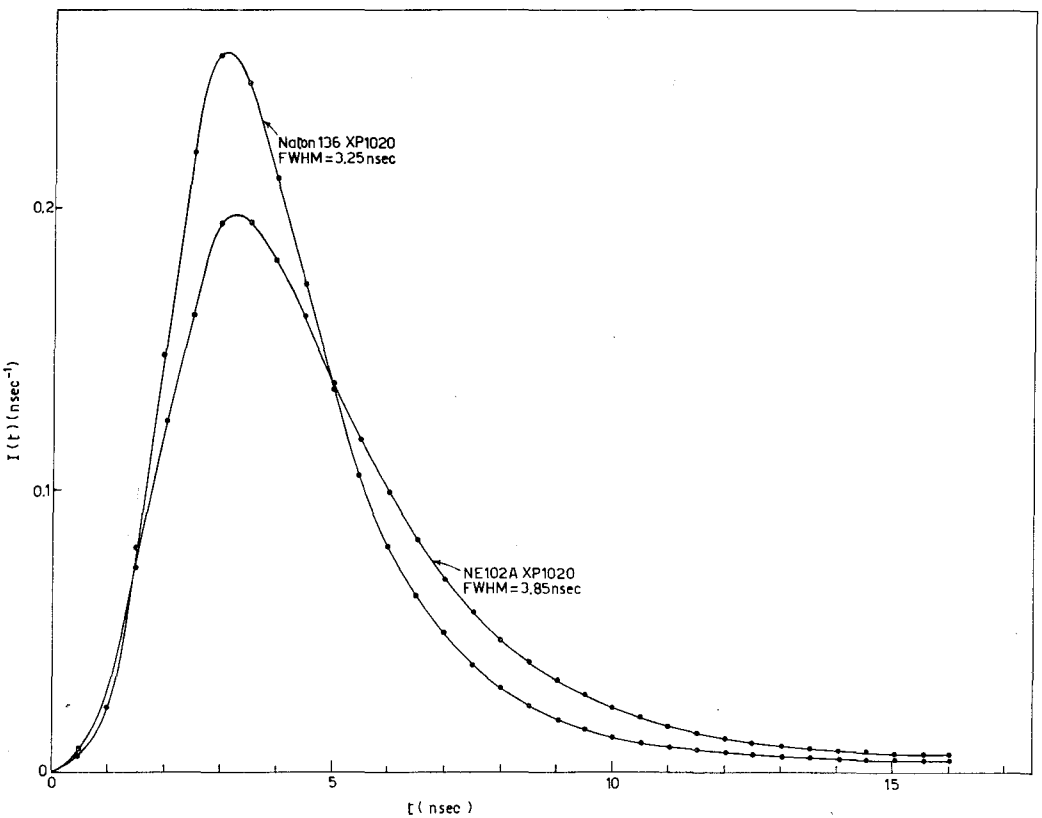

Fig. 1. Equivalent illumination of: A – a $1'' \times 1\frac{1}{2}''$ NE102A scintillator coupled to an XP1020 photomultiplier (HV = 2000 V). Excitation source: ^{60}Co γ-rays. B – a $1'' \times 1\frac{1}{2}''$ Naton 136 scintillator coupled to an XP1020 photomultiplier (HV = 2000 V). Excitation source: ^{60}Co γ-rays.

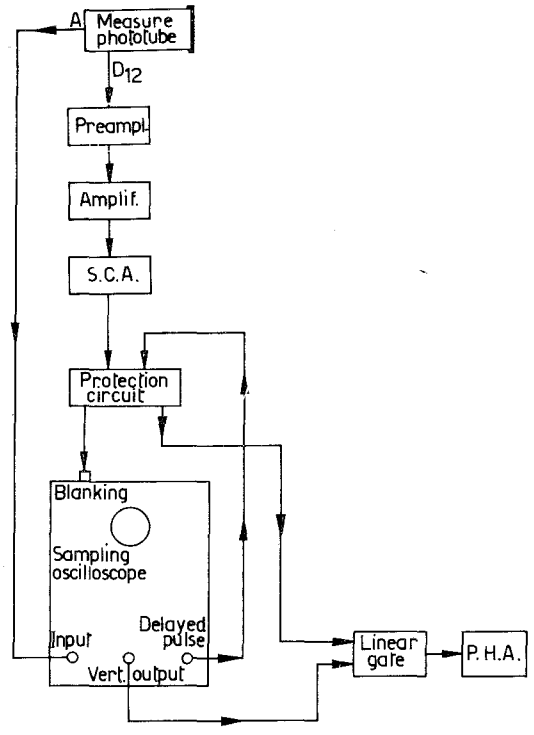

Fig. 2. Block diagram for the measurement of the photomultiplier single electron response (SER).

Finally, we measured directly both $\bar{S}(t)$ and $\varepsilon_S^2(t)$; these two experimental data have been compared with the results obtained from the introduction of the various measured parameters into eqs. (1a) and (2a).

3. Experimental techniques

The equivalent illumination $I(t)$ has been measured using the method introduced by Bollinger and Koechlin[5,6]).

This method gives $I(t)$ as the convolution of the equivalent illumination with the resolution function characteristic of the detecting system that gives the zero time. This last function may be evaluated by means of a prompt coincidence measurement performed using a second identical channel. In our case this function can be characterized by a fwhm less than 200 ps; therefore, for scintillators like the considered ones, having a decay time greater than 1 ns, its contribution can be neglected and the measured $I(t)$ can be taken as identical to the defined equivalent illumination.

Fig. 1 shows the equivalent illuminations, for γ-excitation, of NE102A and Naton 136 scintillators coupled to an XP1020 photomultiplier.

To measure the SER $f(t)$ and the output current pulse $S(t)$ a sampling technique utilizing a sampling oscilloscope (Tektronix 661) together with a PHA, was used.

The block diagram of the system we utilized for the measurement of the SER is shown in fig. 2. The anode pulse from the photomultiplier is sent directly to the input of the sampling oscilloscope, internally triggered. The pulses coming from the dynode of the photomultiplier are amplitude selected by the SCA, which had previously been set about the mean of the amplitude distribution corresponding to single photoelectrons.

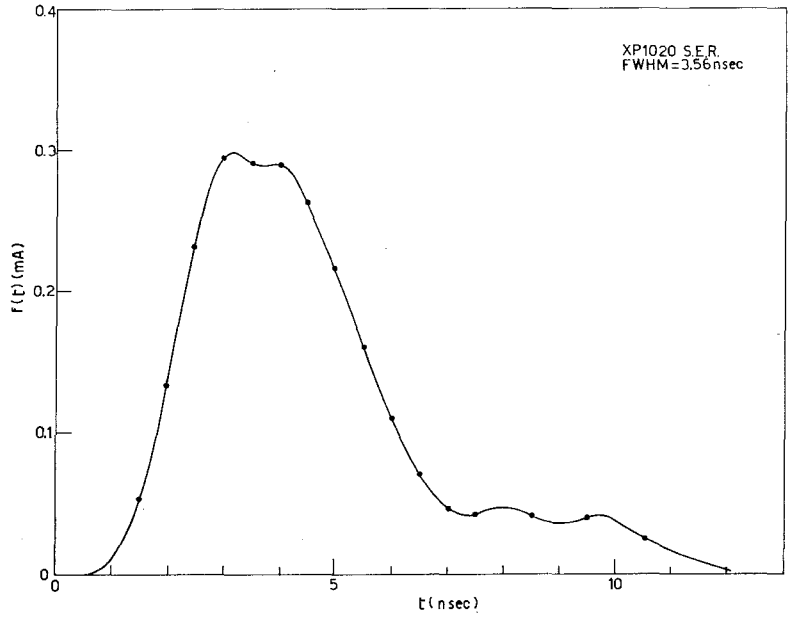

Fig. 3. Experimental $f(t)$ (SER) of the XP1020 photomultiplier (HV = 2000 V). The gain calculated from $f(t)$ area is $A = 7.7 \times 10^6$.

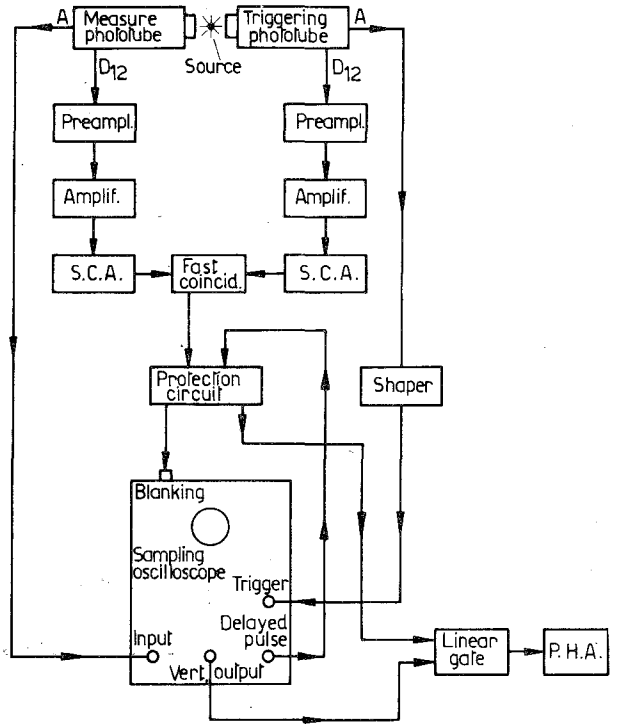

Fig. 4. Block diagram for the measurement of the mean $\bar{S}(t)$ and the variance $\varepsilon_S^2(t)$ of the photomultiplier output current pulse.

This distribution was separately measured poorly coupling a light pulser to the photocathode (less than one photoelectron per light pulse) and analyzing the amplitude spectrum in coincidence[4]).

The coincidence of the output pulse of the SCA with the delayed pulse of the sampling oscilloscope (synchronous with the start of the time base), performed within the protection circuit, gives a signal which samples through a linear gate the vertical output of the oscilloscope. Simultaneously, the output of the protection circuit acts on the unblanking circuit of the oscilloscope so as to present on the screen only those pulses which are sent through the linear gate to the PHA. The protection circuit includes other features ensuring sampling and unblanking operations free from spurious effects. The measurement has been performed at fixed time intervals, (that is at fixed positions on the horizontal axis of the oscilloscope) using the manual scan and analyzing, for every time position, on the PHA the amplitude distribution of the signal.

A typical result obtained in this way is shown in fig. 3. The area of the SER gives directly the gain of the photomultiplier.

A similar system has been used for the measurement of the mean and the variance of the output current pulse (fig. 4). A coincidence method with a ^{22}Na γ-source is used. The anode signal of the auxiliary photomultiplier, triggers the sampling oscilloscope giving the start time. The corresponding delayed pulse, in coincidence with the signal coming from the amplitude selection channels, opens the linear gate and unblanks the oscilloscope.

The amplitude selections are performed on the dynode signals of the two photomultipliers. The SCA

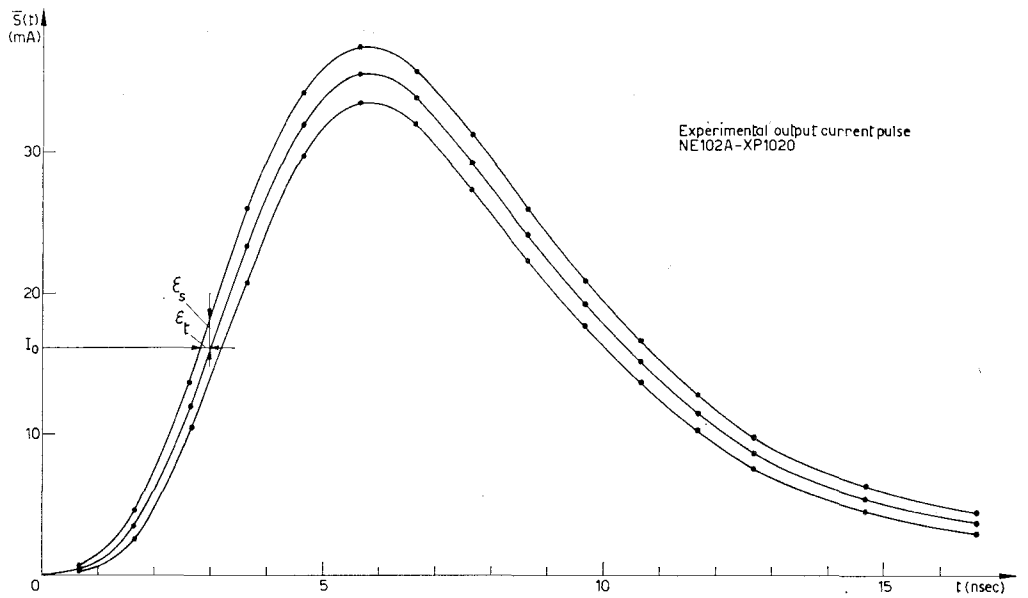

Fig. 5. Experimental output current pulse for an XP1020 photomultiplier (HV = 2000 V) with a $1'' \times 1\frac{1}{2}''$ NE102A scintillator, showing mean and standard deviation for each point. From the area of the mean pulse we obtain $R_f = 243$; the distribution selected by the SCA has a relative variance $\varepsilon_f^2 = 8.33 \times 10^{-4}$. ε_t is the standard deviation for a time measurement done with a threshold crossing at I_0.

on the trigger photomultiplier, coupled to a Naton 136 scintillator, is set on the upper part of the 511 keV Compton edge of the ^{22}Na source.

The SCA on the measure photomultiplier selects a fixed part of the spectrum, so that the position and the window width of this SCA give the values of R_f and ε_f^2 in formulas (1a) and (2a). By selecting a flat zone of the Compton edge, R_f is given by the area of the mean current pulse within the distribution; ε_f^2 is given by $\frac{1}{12}\eta^2$ where η is the relative width of the window. In this case also, the measurement is performed analyzing at fixed time intervals (different positions on the oscilloscope horizontal display) the amplitude distribution of the selected pulses; the mean $\bar{S}(t)$ and the standard deviation $\varepsilon^2(t)$ are then calculated. In fig. 5 we present, for a typical measurement, the mean current pulse $\bar{S}(t)$ and the two limit curves $\bar{S}(t) \pm \varepsilon_S^2(t)$. This representation gives also, by a very straightforward method, the variance of the crossing time of a fixed threshold. For a current threshold I_0, $\varepsilon_t(t)$ is the corresponding standard deviation in the crossing time.

4. Discussion

We wish to point out that the measured mean and variance can not be directly compared to those given by eqs. (1a) and (2a). This because the measured mean pulse shape results from the convolution of the real mean shape of the photomultiplier output pulse with the delay time distribution of the triggering system.

This distribution has a standard deviation of about 150 ps, so that the measured mean shape is practically coincident with the true one. However, when the variance of the pulse amplitude at a fixed time is being measured, this triggering time dispersion may lead to significant effects. This dispersion may be thought as a random translation of the measured pulses on the time axis, characterized by a distribution which is that of the triggering time. This effect contributes to $\varepsilon_t^2(t)$ with a term constant for any time position along the current pulse.

The measured variance in the pulse amplitude, then differs from the true one by a term proportional to the slope of the mean pulse shape.

The experimentally measured $I(t), f(t)$, R_f, ε_f^2 and ε_A^2 allow us to calculate, by means of a digital computer, through eqs. (1a) and (2a), the mean and the variance of the output current pulse. So a comparison between computed and experimental data is possible. This comparison was made for a XP1020 photomultiplier coupled to different scintillators, with various values of the mean photoelectron number R_f and of the relative variance ε_f^2. The computed mean pulse shape and the corresponding experimental points are shown in fig. 6 for a NE102A plastic scintillator, at $R_f = 226$ and $\varepsilon_f^2 = 8.33 \times 10^{-4}$; in fig. 7 for NE102A at $R_f = 111$ and $\varepsilon_f^2 = 8.33 \times 10^{-4}$; in fig. 8 for Naton 136 at $R_f = 262$ and $\varepsilon_f^2 = 3.33 \times 10^{-3}$.

The computed relative standard deviation $\varepsilon_{S\,\mathrm{rel}}(t) =$

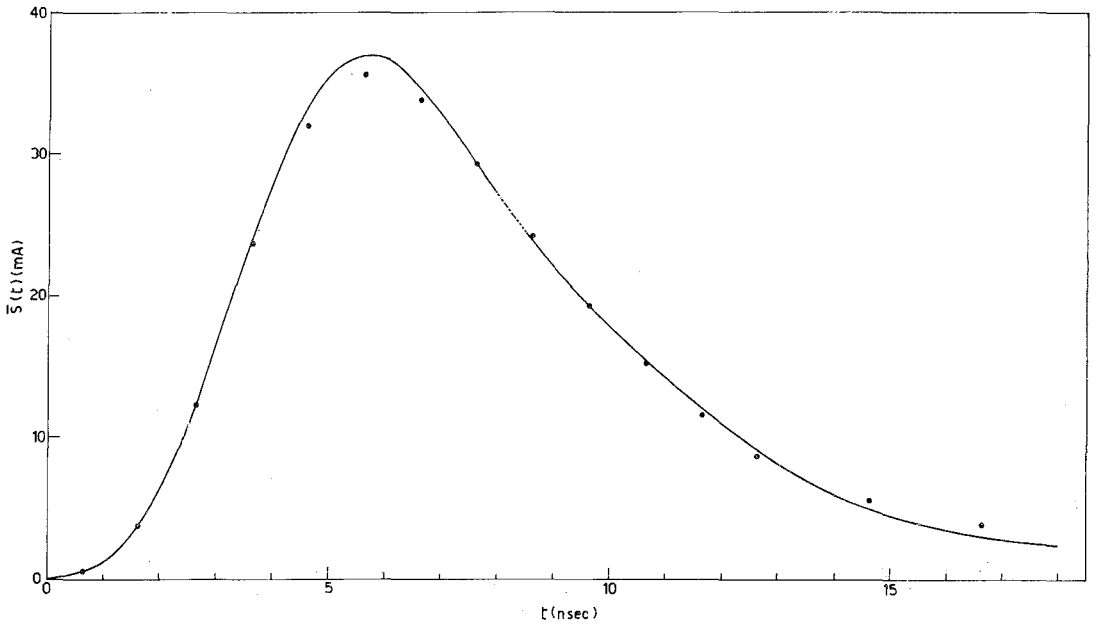

Fig. 6. Calculated mean output current pulse and associated experimental points of an XP1020 photomultiplier (HV = 2000 V) with a $1'' \times 1\frac{1}{2}''$ NE102A scintillator, for a SCA selection with mean number of photoelectrons $R_f = 226$.

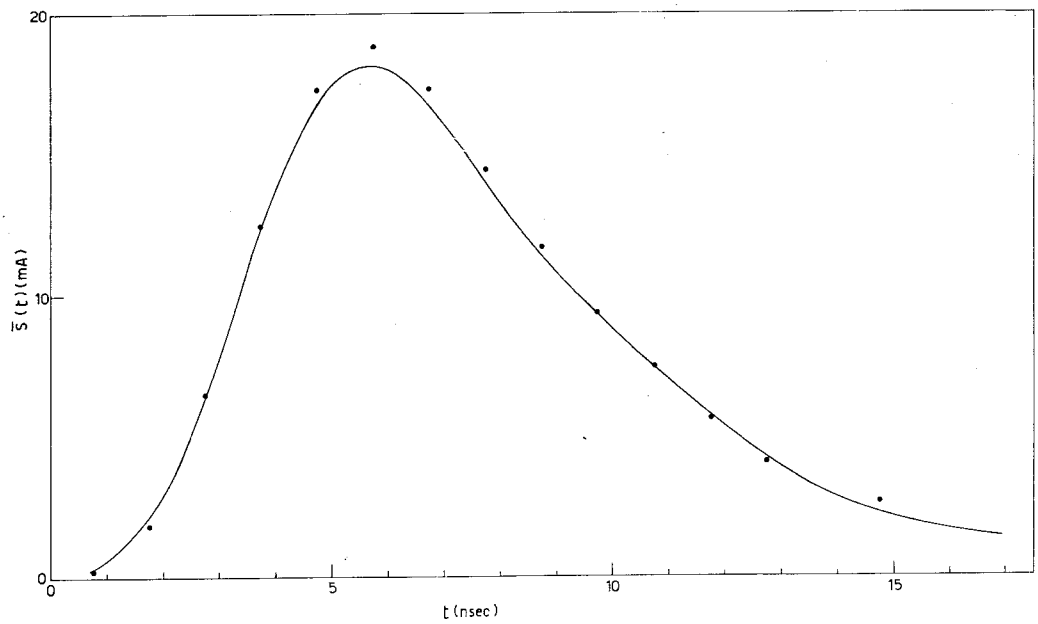

Fig. 7. Calculated mean output current pulse and associated experimental points of an XP1020 photomultiplier (HV = 2000 V) with a $1'' \times 1\frac{1}{2}''$ NE102A scintillator, with mean number of photoelectrons $R_f = 111$.

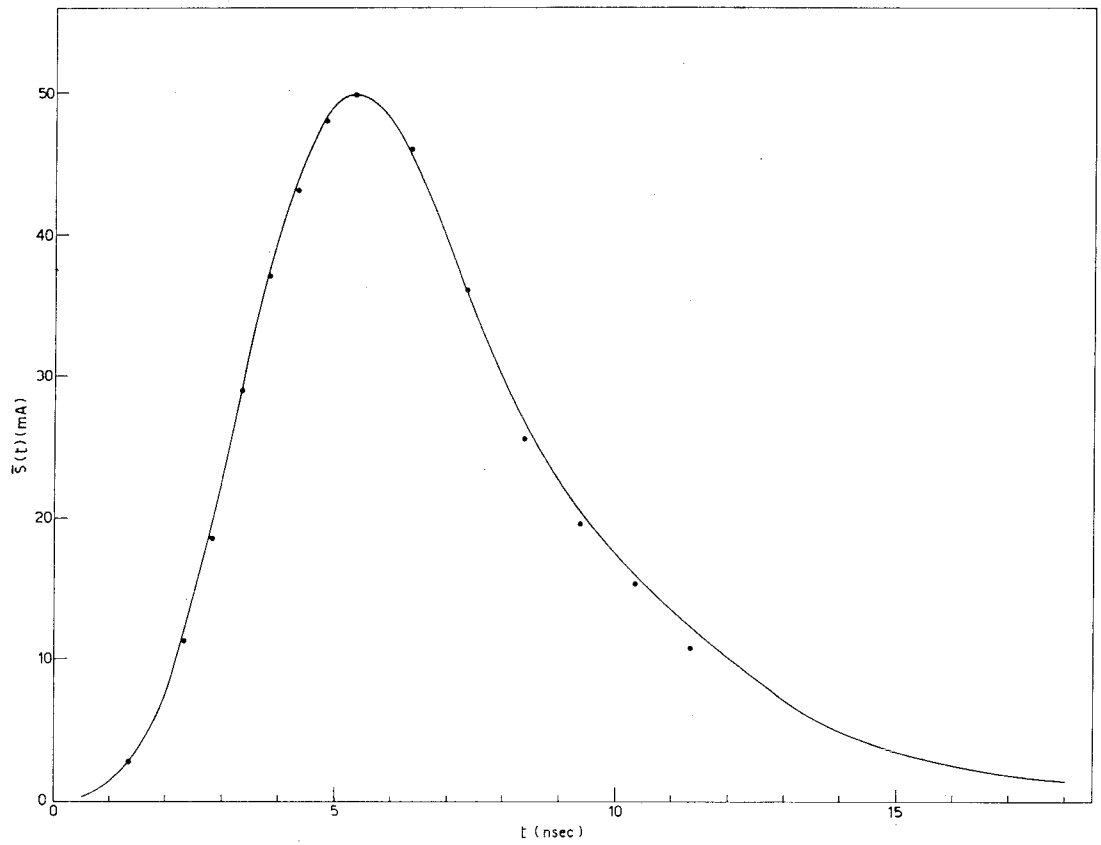

Fig. 8. Calculated mean output current pulse and associated experimental points of an XP1020 photomultiplier (HV = 2000 V) with a $1'' \times 1\frac{1}{2}''$ Naton 136 scintillator, with mean number of photoelectrons $R_f = 262$.

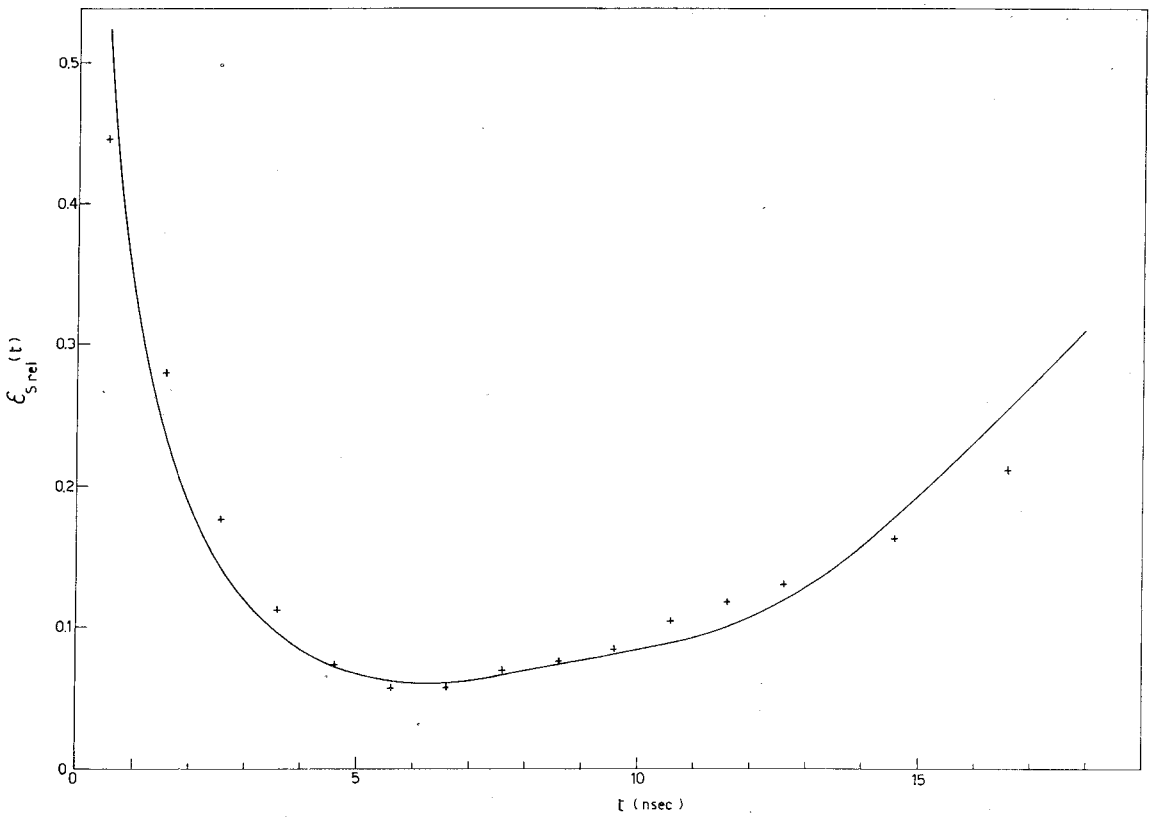

Fig. 9. Relative standard deviation of the output current pulse; calculated results and experimental points. Results refer to the same experimental conditions as in fig. 6; $\varepsilon_f^2 = 8.33 \times 10^{-4}$.

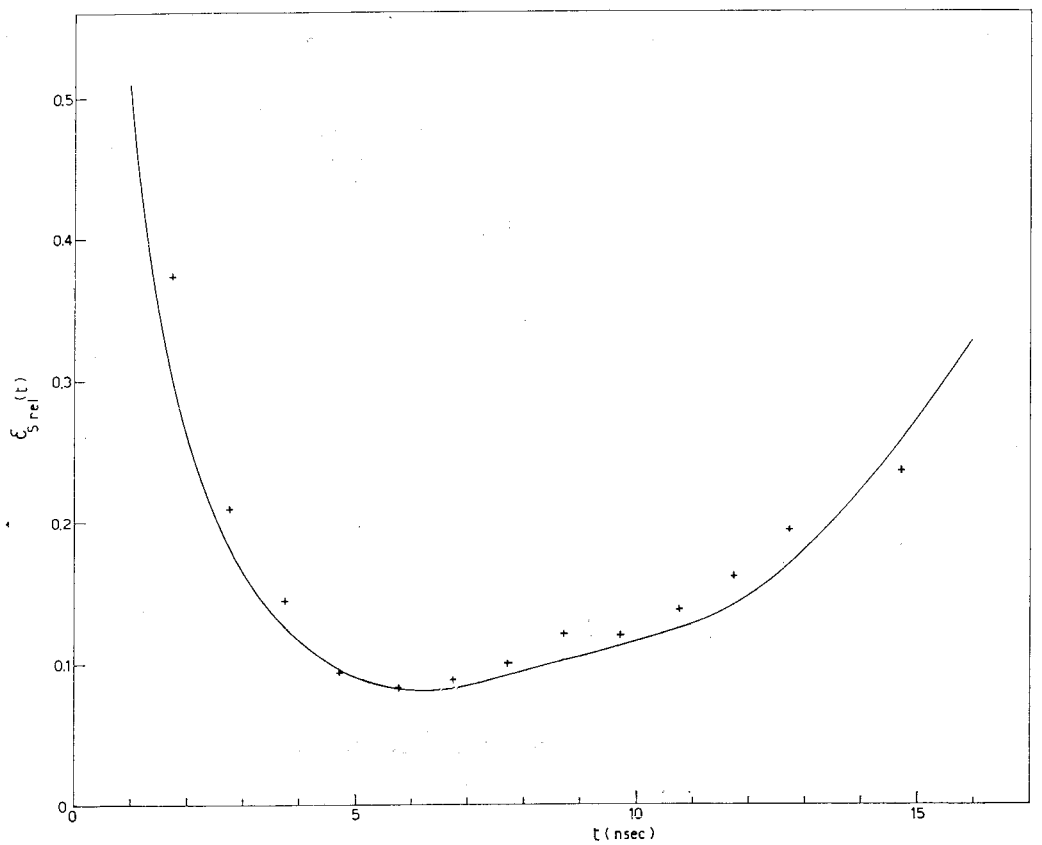

Fig. 10. Relative standard deviation of the output current pulse; calculated results and experimental points. Results refer to the same experimental conditions as in fig. 7; $\varepsilon_f^2 = 8.33 \times 10^{-4}$.

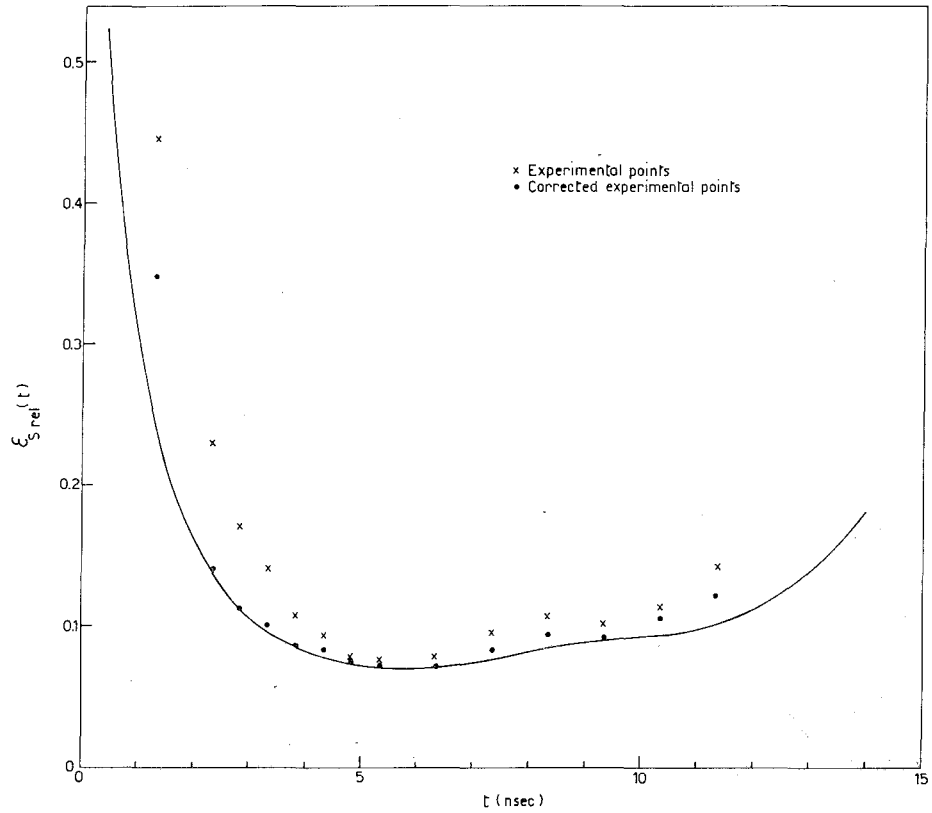

Fig. 11. Relative standard deviation of the output current pulse; calculated results and experimental points. Results refer to the same experimental conditions as in fig. 8; $\varepsilon_f^2 = 3.33 \times 10^{-3}$. The star points refer to the measured values; black points are the experimental values corrected for the triggering jitter assumed equal to $\varepsilon_t = 0.16$ nsec.

$\varepsilon_S(t)/S(t)$ and the corresponding experimental values for the three cases considered are shown in figs. 9, 10 and 11 respectively.

The good agreement between experimental and computed values for the mean pulse shape is evident.

As far as the standard deviation is concerned the agreement is good, in all cases, for values around the peak of the pulse, while there is an appreciable dif-

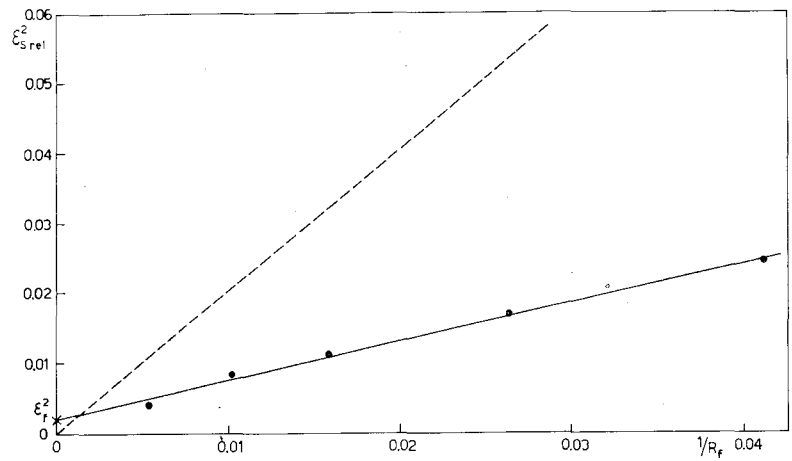

Fig. 12. Relative amplitude variance against $1/R_f$, for the output current pulse of the NE102A–XP1020 (HV = 2000 V) scintillation detector for a fixed value of t: calculated results and experimental points. The SCA relative variance is $\varepsilon_f^2 = 1.88 \times 10^{-3}$. Dotted line is the relative amplitude variance calculated in the same conditions, but with Poisson distributed R_f.

ference for the other points, particularly in the case of Naton 136 at high photoelectron number R_f. As a matter of fact, the jitter in the triggering time gives no contribution to the measured variance for the points where the mean pulse has zero slope, while it contributes appreciably, along the pulse leading and trailing edge: this contribution is particularly evident where the time variance of the current pulse is comparable to that of the triggering time from the auxiliary photomultiplier, which is just the case for Naton 136 with high $R_f = 262$.

For this case we have corrected the experimental values, taking into account this effect: in fig. 11 both the uncorrected and the corrected experimental values are compared with the computed curve.

The dependence of the variance on R_f as given by eq. (2a), has also been experimentally checked by measuring it, at a fixed time position just on the pulse peak, for various R_f, with the other parameters held fixed. The experimental results are shown in fig. 12 to be in good agreement with the ones calculated from eq. (2a). The theoretical straight line corresponding to the Poissonian case, without SCA selection, is also drawn in the same figure (dotted line). The values given by this line correspond to the first term on the right hand side of eq. (2a). It is worthwhile to note the drastic change of the relative variance, on the peak of the output current pulse, from the Poissonian case compared to that with SCA selection.

To take into account with a single parameter $F = \{R_f \varepsilon_f^2/(1+\varepsilon_A^2)\} - 1$, the effect on $\varepsilon_S^2(t)$ of R_f, ε_f^2 and ε_A^2, let us use eq. (1a) to rewrite eq. (2a) as follows:

$$\{R_f \varepsilon_{S\,\mathrm{rel}}^2(t)\}/(1+\varepsilon_A^2) = \left\{ \left[\int_0^t I(\tau) f^2(t-\tau)\,\mathrm{d}\tau \right] \Big/ \left[\int_0^t I(\tau) f(t-\tau)\,\mathrm{d}\tau \right]^2 \right\} + F. \quad (4)$$

We plotted in fig. 13 $\{R_f \varepsilon_{S\,\mathrm{rel}}^2(t)\}/(1+\varepsilon_A^2)$ against t, taking F as a parameter; the values used in eq. (4) for $f(t)$ and $I(t)$ refer to the XP1020 – Naton 136 scintillation detector.

To read correctly the variance values, the zero of the y-scale must be shifted according to the F values. The reduction in variance is marked near the pulse peak, while it is less on the leading and trailing edges.

In a time measurement with plastic scintillators and fast-slow arrangement, the time resolution as a function of R_f when employing a fixed fraction of the current pulse, is given by an expression of the type:

$$\varepsilon_t^2 = a + b/R_f.$$

This may be easily deduced from eq. (3) and eq. (2a).

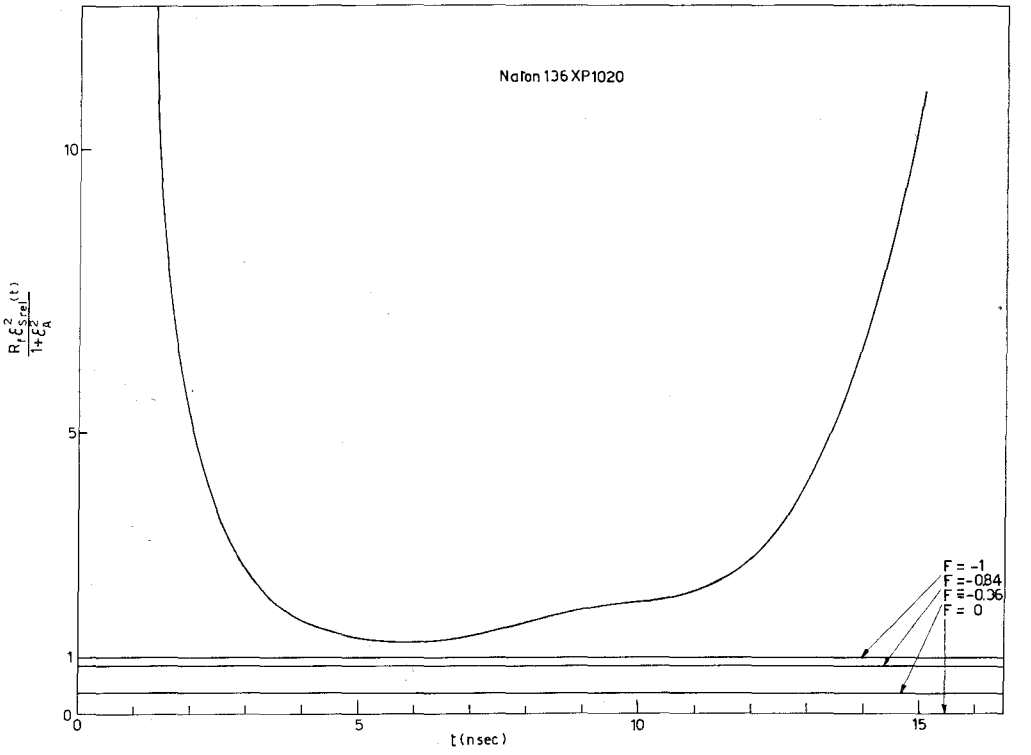

Fig. 13. Standardized relative variance $R_f \varepsilon^2{}_{S\,\mathrm{rel}}(t)/(1+\varepsilon_A{}^2)$ against time t, calculated for the experimental conditions of fig. 11. Various time-axis are given for different values of the parameter $F = [R_f \varepsilon^2{}_{S\,\mathrm{rel}}/(1+\varepsilon_A{}^2)] - 1$ to show the influence of output pulse selection.

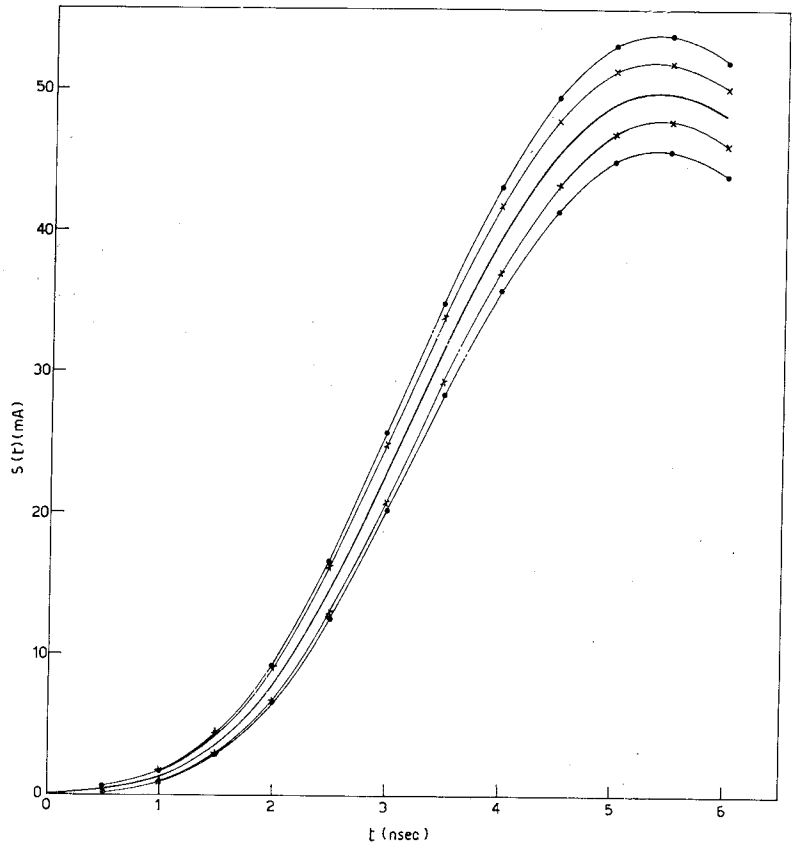

Fig. 14. Pulse leading edge calculated for the experimental conditions of fig. 11, showing the mean value $\bar{S}(t)$ and the upper-lower limits $\bar{S}(t) \pm \varepsilon_S(t)$ for an extremely narrow SCA selection, (i.e. $\varepsilon_f^2 = 0$) (star points) and the corresponding Poissonian case (circle points).

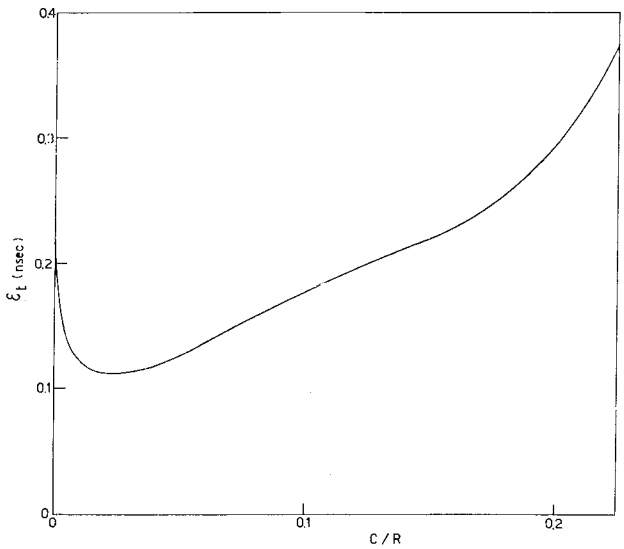

Fig. 15. Threshold crossing time standard deviation as a function of C/R, where C/R is the fraction of the charge collected. Naton 136–XP1020, $R_f = 262$ (figs. 8 and 11).

To make more evident the difference in time resolution between the case of amplitude selection with infinitely narrow channel width (i.e. $\varepsilon_f^2 = 0$) and the hypothetical case of a Poisson distributed number of photoelectrons (which we have already referred to as the Poissonian case), we refer to fig. 14. The mean pulse shape and standard deviation curves are shown for the two cases: it is clearly seen that the difference becomes more and more apparent for increasing time along the pulse leading edge.

For the case of Naton 136–XP1020 with $R_f = 262$ (that is the same considered in figs. 8 and 11), we have calculated the threshold crossing time standard deviation ε_t as a function of C/R, where C/R is the fraction of the charge collected (fig. 15). This curve may be compared with the similar ones considered in previous works on time resolution[1,2,7]). With different scintillation detector parameters this case corresponds to the one considered by Hyman et al.[7]) as "straight response".

It is very important to state explicitly that the theory employed does not take into account space charge and saturation effects in the photomultiplier: therefore to compare experimental data with theoretical results the photomultiplier has to be operated in the linear range.

The authors would like to thank prof. E. Gatti for many stimulating discussions.

Appendix

We will derive eqs. (1a) and (2a) of the text in several steps. First of all, let us calculate mean $\bar{N}(t|N_\infty)$ and covariance $K_N(t,t'|N_\infty)$ of the random function $N(t|N_\infty)$, number of electrons collected, in the interval 0–t, at the output of a multiplying structure for an event at $t=0$, under the condition that the total number of electrons collected is N_∞, i.e. $N(\infty|N_\infty)\equiv N_\infty$. The model for the multiplying structure we will use here, is a cascade of multiplying electrodes and transit time[3]).

For the scintillation detector, electrode 0 is the scintillator, electrode 1 is the photocathode, electrode $2,\ldots,n-1$, are the dynodes of the multiplying structure.

If we know the generating function (g.f.) $\Phi^*(r,t;s,t'|N_\infty)$ associated to the conditional probability $p^*(n_1,t;n_2,t'|N_\infty)$ of collecting at the output of the multiplying structure n_1 electrons in the interval 0–t *and* n_2 in the interval 0–t' *knowing* that N_∞ electrons will be collected in the interval 0–∞, so defined:

$$\Phi^*(r,t;s,t'|N_\infty)=\sum_{n_1=0}^{\infty}\sum_{n_2=0}^{\infty}p^*(n_1,t;n_2,t'|N_\infty)r^{n_1}s^{n_2}, \tag{A1}$$

then, we can at once calculate $\bar{N}(t|N_\infty)$ and $K_N(t,t'|N_\infty)$ from the known eqs.[3]):

$$\bar{N}(t|N_\infty)=\{\partial\Phi^*(r,t;s,t'|N_\infty)/\partial r\}|_{r=s=1}, \tag{A2}$$

$$K_N(t,t'|N_\infty)=\{\partial^2\Phi^*(r,t;s,t'|N_\infty)/\partial r\partial s\}|_{r=s=1}-\bar{N}(t|N_\infty)\bar{N}(t'|N_\infty). \tag{A3}$$

Now, we can obtain the conditional probability $p^*(n_1,t;n_2,t'|N_\infty)$ from the corresponding joint probability $p(n_1,t;n_2,t';N_\infty)$, that is the probability that n_1 electrons are collected at the output in the interval 0–t, n_2 in 0–t' and N_∞ in 0–∞, by means of the formula:

$$p^*(n_1,t;n_2,t'|N_\infty)=p(n_1,t;n_2,t';N_\infty)/p_0(N_\infty), \tag{A4}$$

where $p_0(N_\infty)$ is the probability of collecting at the output N_∞ electrons in 0–∞ time interval.

By introducing the g.f. $\Phi(r,t;s,t';v)$ associated to the joint probability $p(n_1,t;n_2,t';N_\infty)$, so defined:

$$\Phi(r,t;s,t';v)=\sum_{n_1=0}^{\infty}\sum_{n_2=0}^{\infty}\sum_{N_\infty=0}^{\infty}p(n_1,t;n_2,t';N_\infty)r^{n_1}s^{n_2}v^{N_\infty}, \tag{A5}$$

we can find, by substituting eq. (A4) in eq. (A1) and taking into account eq. (A5), that the following equation holds:

$$\Phi^*(r,t;s,t'|N_\infty)=\{1/p_0(N_\infty)\}\,\mathrm{coeff}_{v^{N_\infty}}\,\Phi(r,t;s,t';v). \tag{A6}$$

In eq. (A6) $\mathrm{coeff}_{v^{N_\infty}}$ means the N_∞^{th} coefficient of the expansion of the g.f. $\Phi(r,t;s,t';v)$ in power series of v.

By means of a simple calculation, generalizing the one performed on the bivariate g.f. in[3]), we can find that:

$$\Phi(r,t;s,t';v)=M_0\{f_0(t)*M_1[f_1(t)*\ldots*M_{n-1}(\Phi_{n-1}(r,t;s,t';v))]\}, \tag{A7}$$

where

$$\Phi_{n-1}(r,t;s,t';v)=\{v[1-F_{n-1}(t')]+sv[F_{n-1}(t')-F_{n-1}(t)]+rsvF_{n-1}(t)\}\mathbf{1}(t'-t)+$$
$$+\{v[1-F_{n-1}(t)]+rv[F_{n-1}(t)-F_{n-1}(t')]+rsvF_{n-1}(t')\}\mathbf{1}(t-t'),$$

and: $M_i(s)$ $(i=0,\ldots,n-1)$ are the g.f. related to the multiplication factor distribution at the electrode i; $f_i(t)$ $(i=0,\ldots,n-1)$ are the probability density functions of flight time between electrodes i and $i+1$; $F_{n-1}(t)=\int_0^t f_{n-1}(\tau)\mathrm{d}\tau$; $\mathbf{1}(t)$ is the step function; $*$ stands for the convolution integral so defined:

$$p(t)*q(t,t')=\int_0^{\infty}p(\tau)q(t-\tau,t'-\tau)\,\mathrm{d}\tau.$$

By introducing eq. (A7) in eqs. (A2) and (A3) we obtain the expressions for $\bar{N}(t\,|\,N_\infty)$ and $K_N(t,t'\,|\,N_\infty)$:

$$\bar{N}(t\,|\,N_\infty) = a f_0(t) * \ldots * f_{n-2}(t) * F_{n-1}(t), \tag{A8}$$

$$\begin{aligned} K_N(t,t'\,|\,N_\infty) = {} & (b_0 - a^2)[f_0(t) * \ldots * f_{n-2}(t) * F_{n-1}(t)][f_0(t') * \ldots * f_{n-2}(t') * F_{n-1}(t')] + \\ & + \sum_{k=1}^{n-1} b_k f_0(t) * \ldots * f_{k-1}(t) * [f_k(t) * \ldots * f_{n-2}(t) * F_{n-1}(t)][f_k(t') * \ldots * f_{n-2}(t') * F_{n-1}(t')] + \\ & + a\{[f_0(t) * \ldots * f_{n-2}(t) * F_{n-1}(t)]\mathbf{1}(t'-t) + [f_0(t') * \ldots * f_{n-2}(t') * F_{n-1}(t')]\mathbf{1}(t-t')\}, \end{aligned} \tag{A9}$$

where

$$\begin{aligned} a = {} & \{1/p_0(N_\infty)\}\ \text{coeff}_{v^{N_\infty}}\{v\,\mathrm{d}M_0[M_1 \ldots M_{n-2}(M_{n-1}(v))]/\mathrm{d}v\} \\ & = \{1/p_0(N_\infty)\}\,\text{coeff}_{v^{N_\infty}}\left\{v\left[\sum_{N=1}^{\infty} N p_0(N) v^{N-1}\right]\right\} = N_\infty, \end{aligned} \tag{A10}$$

$$\begin{aligned} b_k = {} & \frac{1}{p_0(N_\infty)}\ \text{coeff}_{v^{N_\infty}}\left\{\frac{\mathrm{d}M_0[M_1 \ldots M_{n-2}(M_{n-1}(v))]}{\mathrm{d}v} \cdot \right. \\ & \cdot \frac{\partial^2 M_k[M_{k+1} \ldots M_{n-2}(M_{n-1}(v))]/\partial[M_{k+1} \ldots M_{n-2}(M_{n-1}(v))]^2}{\partial M_k[M_{k+1} \ldots M_{n-2}(M_{n-1}(v))]/\partial[M_{k+1} \ldots M_{n-2}(M_{n-1}(v))]} \cdot \\ & \left. \cdot \frac{\mathrm{d}M_{k+1}[M_{k+2} \ldots M_{n-2}(M_{n-1}(v))]}{\mathrm{d}v} \cdot v^2 \right\}. \end{aligned} \tag{A11}$$

From eq. (A11) it is easy to verify that a relation exists between the b_k's:

$$\sum_{k=0}^{n-1} b_k = \frac{1}{p_0(N_\infty)}\,\text{coeff}_{v^{N_\infty}}\left\{\frac{\mathrm{d}^2 M_0[M_1 \ldots M_{n-2}(M_{n-1}(v))]}{\mathrm{d}v^2} v^2\right\} = N_\infty(N_\infty - 1),$$

from which we can obtain b_0 as a function of $b_k (k = 1,\ldots,n-1)$:

$$b_0 = N_\infty(N_\infty - 1) - \sum_{k=1}^{n-1} b_k. \tag{A12}$$

Eqs. (A10) and (A12) follow being $N(\infty\,|\,N_\infty) \equiv N_\infty$, therefore $\bar{N}(\infty\,|\,N_\infty) = N_\infty$, $K_N(\infty,\infty\,|\,N_\infty) = 0$.

Taking into account eqs. (A10) and (A12) we can now write eqs. (A8) and (A9) in this way:

$$\bar{N}(t\,|\,N_\infty) = N_\infty f_0(t) * \ldots f_{n-2}(t) * F_{n-1}(t), \tag{A13}$$

$$\begin{aligned} K_N(t,t'\,|\,N_\infty) = {} & -\left(N_\infty + \sum_{k=1}^{n-1} b_k\right)[f_0(t) * \ldots * f_{n-2}(t) * F_{n-1}(t)][f_0(t') * \ldots * f_{n-2}(t') * F_{n-1}(t')] + \\ & + \sum_{k=1}^{n-1} b_k f_0(t) * \ldots * f_{k-1}(t) * [f_k(t) * \ldots * f_{n-2}(t) * F_{n-1}(t)][f_k(t') * \ldots * f_{n-2}(t') * F_{n-1}(t')] + \\ & + N_\infty\{[f_0(t) * \ldots * f_{n-2}(t) * F_{n-1}(t)]\mathbf{1}(t'-t) + [f_0(t') * \ldots * f_{n-2}(t') * F_{n-1}(t')]\mathbf{1}(t-t')\}. \end{aligned} \tag{A14}$$

$\bar{N}(t\,|\,N_\infty)$ and $K_N(t,t'\,|\,N_\infty)$ are the mean and covariance of the random function $N(t\,|\,N_\infty)$ number of electrons collected at the output in the interval 0–t for an event detected at $t = 0$; to obtain mean $\bar{n}(t\,|\,N_\infty)$ and covariance $K_n(t,t'\,|\,N_\infty)$ of the random function $n(t\,|\,N_\infty) = \mathrm{d}N(t\,|\,N_\infty)/\mathrm{d}t$ density of the number of electrons collected at the output, we can apply the known equations:

$$\bar{n}(t\,|\,N_\infty) = \mathrm{d}\bar{N}(t\,|\,N_\infty)/\mathrm{d}t, \qquad K_n(t,t'\,|\,N_\infty) = \partial^2 K_N(t,t'\,|\,N_\infty)/\partial t \partial t'.$$

Taking this into account we obtain:

$$\bar{n}(t\,|\,N_\infty) = N_\infty f_0(t) * \ldots * f_{n-1}(t), \tag{A15}$$

$$\begin{aligned} K_N(t,t'\,|\,N_\infty) = {} & -\left(N_\infty + \sum_{k=1}^{n-1} b_k\right)[f_0(t) * \ldots * f_{n-1}(t)][f_0(t') * \ldots * f_{n-1}(t')] + \\ & + \sum_{k=1}^{n-1} b_k f_0(t) * \ldots * f_{k-1}(t) * [f_k(t) * \ldots * f_{n-1}(t)][f_k(t') * \ldots * f_{n-1}(t')] + \\ & + N_\infty f_0(t) * \ldots * f_{n-1}(t)\delta(t'-t). \end{aligned} \tag{A16}$$

If there is a linear filter, having $f_n(t)$ as $\delta(t)$-response, cascaded to the multiplying structure, mean and covariance of the output of this filter become[3]):

$$\bar{n}(t\,|\,N_\infty) = N_\infty f_0(t) * \ldots * f_n(t), \tag{A17}$$

$$\begin{aligned} K_n(t,t'\,|\,N_\infty) = &-(N_\infty + \sum_{k=1}^{n-1} b_k)[f_0(t) * \ldots * f_n(t)]\,[f_0(t') * \ldots * f_n(t')] + \\ &+ \sum_{k=1}^{n-1} b_k f_0(t) * \ldots * f_{k-1}(t) * [f_k(t) * \ldots * f_n(t)]\,[f_0(t') * \ldots * f_n(t')] + \\ &+ N_\infty f_0(t) * \ldots * f_{n-1}(t) * f_n(t) f_n(t'). \end{aligned} \tag{A18}$$

From eq. (A18), putting $t = t'$ we obtain the amplitude variance $\varepsilon_n^2(t\,|\,N_\infty)$:

$$\begin{aligned} \varepsilon_n^2(t\,|\,N_\infty) = &-\left(N_\infty + \sum_{k=1}^{n-1} b_k\right)[f_0(t) * \ldots * f_n(t)]^2 + \sum_{k=1}^{n-1} b_k f_0(t) * \ldots * f_{k-1}(t) * [f_k(t) * \ldots * f_n(t)]^2 + \\ &+ N_\infty f_0(t) * \ldots * f_{n-1}(t) * f_n^2(t). \end{aligned} \tag{A19}$$

To evaluate the coefficients b_k's given by eqs. (A11) in an interesting case, let us assume a Bernoulli trial with success probability p the multiplication at the photocathode (electrode 1), i.e. $M_1(s) = (1-p)+ps$, and Poisson-distributed with mean value g_k the multiplications at the dynodes (electrodes $2,\ldots,n-1$), i.e.

$$\mathrm{d}^2 M_k(s)/\mathrm{d}s^2 = g_k \mathrm{d}M_k(s)/\mathrm{d}s = g_k^2 M_k(s), \qquad (k = 2,\ldots,n-1).$$

With those assumptions, we obtain: $b_1 = 0,$ (A20)

$$b_k = \frac{g_k}{p_0(N_\infty)}\ \mathrm{coeff}_{\,v^{N_\infty}} \left\{ \frac{\mathrm{d}M_0[M_1 \ldots M_{n-2}(M_{n-1}(v))]}{\mathrm{d}v} \cdot \frac{\mathrm{d}M_{k+1}[M_{k+2} \ldots M_{n-2}(M_{n-1}(v))]}{\mathrm{d}v} \cdot v^2 \right\}, \ (k = 2,\ldots,n-1). \tag{A21}$$

Let us note that $M_0[M_1 \ldots M_{n-2}(M_{n-1}(v))]$ and $M_{k+1}[M_{k+2} \ldots M_{n-2}(M_{n-1}(v))]$ are the g.f. associated to the probability distributions $p_0(N)$ and $p_{k+1}(N')$ of collecting, at the output, a total number N and N' for an event impinging on the electrodes 0 and $k+1$ respectively [eq. (A7) with $t = t' = \infty$]. According to the definition of generating function, we can so rewrite eq. (A21) in the form:

$$\begin{aligned} b_k &= \{g_k/p_0(N_\infty)\}\ \mathrm{coeff}_{\,v^{N_\infty}} [(\sum_{N=1}^{\infty} N p_0(N) v^{N-1})(\sum_{N'=1}^{\infty} N' p_{k+1}(N') v^{N'-1}) v^2] \\ &= \{g_k/p_0(N_\infty)\} \sum_{N'=0}^{N_\infty} (N_\infty - N') p_0(N_\infty - N') N' p_{k+1}(N'), \qquad (k = 2,\ldots,n-1). \end{aligned} \tag{A22}$$

An exact calculation of b_k requires the knowledge of $p_0(N)$ and $p_{k+1}(N')$; we know the corresponding generating functions but it is very cumbersome to find them out. Therefore we will only show that, with good approximation, being the N' values for which $p_{k+1}(N')$ is different from zero much less than the interesting N_∞ values, $N_\infty - N' \simeq N_\infty$ and $p_0(N_\infty - N') \simeq p_0(N_\infty)$. In fact, it is easy to calculate the ratios $\bar{N}'/\bar{N}_\infty$ and $\varepsilon_{N'}^2/\varepsilon_{N_\infty}^2$ of the means and the variances of the distributions defined by $p_{k+1}(N')$ and $p_0(N)$:

$$\frac{N'}{\bar{N}_\infty} = \left.\frac{\mathrm{d}M_{k+1}[M_{k+2} \ldots M_{n-2}(M_{n-1}(v))]/\mathrm{d}v}{\mathrm{d}M_0[M_1 \ldots M_{n-2}(M_{n-1}(v))]/\mathrm{d}v}\right|_{v=1} = \frac{1}{g_0 p g_2 \ldots g_k}, \qquad (k = 2,\ldots,n-1),$$

$$\frac{\varepsilon_{N'}^2}{\varepsilon_{N_\infty}^2} = \frac{\mathrm{d}^2 M_{k+1}[M_{k+2} \ldots M_{n-2}(M_{n-1}(v))]/\mathrm{d}v^2\,|_{v=1} - \bar{N}'^2 + \bar{N}'}{\mathrm{d}^2 M_0[M_1 \ldots M_{n-2}(M_{n-1}(v))]/\mathrm{d}v^2\,|_{v=1} - \bar{N}_\infty^2 + \bar{N}_\infty} \leqq \frac{1}{g_0 p g_2^2 \ldots g_k^2}, \qquad (k = 2,\ldots,n-1).$$

In practical cases, as $g_0 p g_2$ is never less than 30, we can conclude that the distribution defined by $p_0(N)$ has a mean value and a width greater than the ones defined by $p_{k+1}(N)$, so our hypothesis holds; eq. (A22) then becomes:

$$b_k = N_\infty g_k \ldots g_{n-1}, \qquad (k = 2,\ldots,n-1) \tag{A23}$$

and from this, substituting eq. (A20) and (A23) into eq. (A19) we obtain:

$$\varepsilon_n^2(t\,|\,N_\infty) = -N_\infty g_2 \dots g_{n-1}\left(1+\frac{1}{g_2}+\frac{1}{g_2 g_3}+\dots+\frac{1}{g_2\dots g_{n-1}}\right)[f_0(t)*\dots*f_n(t)]^2 +$$

$$+N_\infty \sum_{k=2}^{n-1} g_k \dots g_{n-1} f_0(t)*\dots*f_{k-1}(t)*[f_k(t)*\dots*f_n(t)]^2 + N_\infty f_0(t)*\dots*f_{n-1}(t)*f_n^2(t). \quad \text{(A24)}$$

Since the pdf $f_i(t)$ are not easily measurable and also to simplify the rather involved formula (A24) let us approximate, as in previous works[1,2]), to unity the ratios

$$\frac{f_0(t)*\dots*f_{k-1}(t)*[f_k(t)*\dots*f_n(t)]^2}{f_0(t)*f_1(t)*[f_2(t)*\dots*f_n(t)]^2}, \qquad (k=2,\dots,n).$$

With this further hypothesis, by indicating with $f_0(t)*f_1(t)=I(t)$ the equivalent illumination, with $g_2\dots g_{n-1}\cdot f_2(t)*\dots*f_n(t)=f(t)$ the SER and with

$$\frac{1}{g_2}+\frac{1}{g_2 g_3}+\dots+\frac{1}{g_2\dots g_{n-1}}=\varepsilon_A^2,$$

the electron multiplier gain relative variance, we can rewrite eqs. (A17) and (A24) in this way:

$$\bar{n}(t\,|\,N_\infty) = \{N_\infty/(g_2\dots g_{n-1})\}I(t)*f(t), \quad \text{(A25)}$$

$$\varepsilon_n^2(t\,|\,N_\infty) = \{N_\infty/(g_2\dots g_{n-1})\}(1+\varepsilon_A^2)\{I(t)*f^2(t)-[I(t)*f(t)]^2\}. \quad \text{(A26)}$$

Finally, to obtain mean value $\bar{S}(t)$ and variance $\varepsilon_S^2(t)$ for the output current pulses, whose area N_∞ is distributed with mean value $\bar{N}_\infty$ and variance $\overline{N_\infty^2}-\bar{N}_\infty^2$, we must only sum the weighted contributions as given by eqs. (A25) and (A26). So we obtain:

$$\bar{S}(t) = \{\bar{N}_\infty/(g_2\dots g_{n-1})\}I(t)*f(t), \quad \text{(A27)}$$

$$\varepsilon_S^2(t) = \{\bar{N}_\infty/(g_2\dots g_{n-1})\}(1+\varepsilon_A^2)\{I(t)*f^2(t)-[I(t)*f(t)]^2\}+\{(\overline{N_\infty^2}-\bar{N}_\infty^2)/(g_2^2\dots g_{n-1}^2)\}[I(t)*f(t)]^2. \quad \text{(A28)}$$

By indicating with $\bar{N}_\infty/(g_2\dots g_{n-1})=R_f$ the number of photoelectrons corresponding to the mean number $\bar{N}_\infty$ of total collected electrons and with $(\overline{N_\infty^2}-\bar{N}_\infty^2)/\bar{N}_\infty^2=\varepsilon_f^2$ the relative variance of the total number of electron collected at the output, eqs. (A27) and (A28) become:

$$\bar{S}(t) = R_f I(t)*f(t), \quad \text{(A29)}$$

$$\varepsilon_S^2(t) = (1+\varepsilon_A^2)R_f I(t)*f^2(t)+\{\varepsilon_f^2-(1+\varepsilon_A^2)/R_f\}\bar{S}^2(t), \quad \text{(A30)}$$

which coincide with eqs. (1a) and (2a) of the text. With the further hypothesis of Poisson distributed number of photoelectrons[1,2]), that is $\varepsilon_f^2=(1+\varepsilon_A^2)/R_f$, we can see that eqs. (A29) and (A30) give eqs. (1) and (2).

References

1) E. Gatti and V. Svelto, Nucl. Instr. and Meth. **30** (1964) 231.

2) E. Gatti and V. Svelto, Nucl. Instr. and Meth. **43** (1966) 248.

3) S. Donati, E. Gatti and V. Svelto, Nucl. Instr. and Meth. **46** (1967) 165.

4) M. Bertolaccini and S. Cova, Energia Nucleare **10** (1963) 259.

5) L. M. Bollinger and G. E. Thomas, Rev. Sci. Instr. **32** (1961) 1044.

6) Y. Koechlin and A. Raviart, Nucl. Instr. and Meth. **29** (1964) 45.

7) L. G. Hyman, R. M. Schwarcz and R. A. Schluter, Rev. Sci. Instr. **35** (1964) 393.